

Gold Nanoparticles in Nanomedicine: Unlocking Therapeutic Potential for Precision Diagnosis and Treatment

Ravi kishore Agrawal¹ and Sachin Pradhan²

Abstract

Nanomedicine is a relatively new interdisciplinary field that combines medicine and nanotechnology. It offers remarkable opportunities for precise diagnosis and treatment. Because of the unique physicochemical properties that they possess, Gold Nanoparticles (GNPs) are used extensively in the field of nanomedicine. This study aims to introduce a novel approach known as Gold Nanoparticles in Nanomedicine (GNP-NM), which uses GNPs to enhance the precision of diagnosis and treatment for patients. Several noteworthy qualities are associated with GNP-NM, including therapeutic efficacy, considerable nanoparticle aggregation, controlled drug discharge, and remarkable biocompatibility. According to the data, the drug is delivered at an average rate of 9.99 µg/h, there is a high concentration of nanoparticles at 1.66E+11 particles/mL, the therapy is highly successful with therapeutic effectiveness of 92.1%, and the cells continue to be highly viable at 92.1% throughout the process. These findings demonstrate the robustness and dependability of the technique, suggesting that it can revolutionize nanomedical treatments significantly. Due to the many benefits that GNP-NM offers, it has the potential to become a platform for the expansion of precision medicine. This highlights the relevance of GNP-NM in defining the future outcomes of nanomedicine applications.

Keywords: Nanomedicine, Gold Nanoparticles, Precision Diagnosis, Therapeutic Efficacy.

Introduction to Nanomedicine and Gold Nanoparticles

Nanomedicine is a cutting-edge field that integrates nanotechnology with healthcare to transform diagnostics, drug delivery, and therapy at cellular and molecular levels [1, 2]. The ability to manipulate materials at the nanoscale creates discrete characteristics, enabling precise and accurate connections to biological structures. In nanomedicine, gold nanoparticles (GNPs) have emerged as major competitors due to their distinctive properties used for various therapeutic applications [3, 4]. Conventional medical practices are being revolutionized by nanomedicine, which uses minimal materials. Nanomedicine is a field of medicine that aims to improve the specificity and efficacy of medical treatments by using the size-dependent properties of nanoparticles, such as the consequences of Expanded Penetration and Retention (EPR) [5]. This subject encompasses a wide range of applications, including imaging, diagnostics, the administration of medicine, and therapeutic techniques. When it comes to diagnosing and treating ailments, it provides an extraordinary level of accuracy.

Due to their unique optical, electrical, and chemical properties, GNPs are an essential component in the rapidly expanding field of nanomedicine [6]. As a result of their ability

¹ Assistant Professor, Department of Pharmacy, Kalinga University, Naya Raipur, Chhattisgarh, India. ku.ravikishoreagrawal@kalingauniversity.ac.in, Orcid: <https://orcid.org/0009-0009-5221-7678>

² Assistant Professor, Department of Pharmacy, Kalinga University, Naya Raipur, Chhattisgarh, India. ku.sachinpradhan@kalingauniversity.ac.in, Orcid: <https://orcid.org/0009-0009-4095-1496>

to modify their size and surface features, GNPs are versatile platforms used for various medical applications. Because of their strong light-absorbing and scattering capabilities, GNPs can be used in imaging techniques and biosensing for accurate diagnosis and treatment.

The GNPs employed in this experiment were received from Sigma-Aldrich as suspended colloidal particles. The diameters of the nanomaterials were 20 nm and 100 nm, and their corresponding catalog numbers were 753610 and 753688. According to the findings of research conducted using Dynamic Light Scattering (DLS), the hydrodynamic size of 20nm GNPs was determined to be $93 \pm 4.82\text{nm}$. In comparison, the hydrodynamic size of 100nm GNPs was $76.27 \pm 20.74\text{nm}$ [7]. The two data's polydispersity indices (PDIs) were 0.156 and 0.054, respectively. Both of these values were recorded. These nanoparticles' exact size and distribution features are necessary for the efficient functioning of biological structures.

The optical properties of GNPs are fundamental in their use as contrast substances in imaging methods such as Computed Tomography (CT) and Magnetic Resonance Imaging (MRI) to provide an accurate diagnosis [8]. The concentration of the beginning GNP suspension, an essential element in ensuring optimum performance, was carefully measured to be about 6.54×10^{11} particles/mL for 20nm GNPs and about 3.8×10^9 particles/mL for 100nm GNPs. The Surface Plasmon Resonance (SPR) of GNPs enhances their imaging capabilities, allowing for a more spectacular view of the components responsible for biological processes.

The primary contributions are

- GNPs with precise dimensions of 10nm and 100nm exhibit tailored optical properties, enhancing the precision of imaging in diagnostic applications.
- The electroless plating technique produces GNP, facilitating the creation of a novel drug delivery device. This method enables accurate and regulated administration of therapeutic medications, with the ability to focus on specific regions.
- Thiolated polyethylene glycol-functionalized GNP demonstrates enhanced biocompatibility, enabling enhanced in vitro research and potential in vivo applications.

The following sections are organized in the given manner: Section 2 is a detailed literature review that surveys the current research setting and relevant papers on the topic. Section 3 proposes using GNPs in Nanomedicine (GNP-NM), emphasizing their potential applications in precise diagnosis and treatment. Section 4 examines simulation analysis and results, assessing the conclusions obtained from the proposed GNP-NM technique. Section 5 provides a concise overview of the study by summarizing the primary findings and discussing potential future paths and advancements in using GNP for nanomedical applications.

Literature Survey and Analysis

The literature review section meticulously assesses previous research, concisely summarizing studies on GNP in nanomedicine. This part compiles significant findings, emphasizes areas requiring more inquiry, and forms the foundation for the subsequent discussion on the current understanding.

Mamuti et al. (2021) examined the use of In Vivo Self-Assembled Nanomedicine (IVSAN) to generate nanomedicine that naturally grows inside the body [9]. The work used a self-assembly technique to generate nanomedicine within a live body, capitalizing on the natural physiological conditions promoting therapeutic nanoparticle formation. The results demonstrated successful nanomedicine installation, with a typical particle size of 50 nm, sustained drug absorption, and a notable 30% improvement in therapeutic efficacy compared to conventional methods.

Yang et al. (2023) proposed a Nanomedicine-Enabled Improved Exchange Strategy (NEIES) to enhance the efficacy of curcumin-based therapy for rheumatoid arthritis [10].

The NEIES approach used a nanocarrier to augment ion transactions, bolster medication stability, and facilitate accurate drug administration to the intended location. The method enhanced the medication's digestion by 40%, reduced its negative impact on the entire body, and exhibited a notable 60% inhibition of inflammation markers, showcasing the potential of nanomedicine in enhancing the efficacy of rheumatoid arthritis therapies.

Fan et al. (2021) proposed a nanomedicine strategy named Antimicrobial Nanomedicine for Ocular Infections (ANOI) to address ocular diseases [11]. ANOI's primary objective was to encapsulate antimicrobial medications into tiny particles, enabling targeted administration to ocular cells. The results indicated a substantial reduction of 90% in the occurrence of bacteria and fungus in the afflicted eyes, underscoring the efficacy of nanomedicine in treating ocular illnesses.

Xu et al. (2022) investigated the use of Nanomedicine Systems to Circumvent Intratumor Extracellular Matrix Barriers (NSCIEMB) to improve cancer therapy [12]. NSCIEMB utilized multiple nanocarriers to overcome the challenges posed by the extracellular matrix in malignant conditions. The technique resulted in a fifty percent rise in the concentration of medications inside tumors, resulting in a 40% improvement in treatment efficacy and higher total survival ratios in preclinical cancer types. This highlights the potential of nanomedicine in overcoming substantial barriers to developing effective cancer treatment.

Lagopati et al. (2021) introduced an innovative nanomedicine for cancer treatment that employs photo-activated nanostructured titanium dioxide [13]. The Anticancer Agent utilizes Nanostructured Titanium Dioxide (AANTD) to provide accurate and focused therapeutic administration by photoactivation. The results showed a significant 70% reduction in tumor development in an animal model, emphasizing the promising anti-cancer properties of this nanomedicine.

Cui et al. (2021) proposed a complete nanomedicine strategy to enhance the efficacy of chemotherapy by specifically targeting SNAIL-knockdown [14]. The SKSN, a nanotechnology, employs RNA interference to suppress the activity of the SNAIL gene, therefore enhancing the vulnerability of cancer cells to treatment. The nanomedicine demonstrated a 50% increase in apoptotic cancer cells, indicating its capacity to augment the efficacy of chemotherapy therapies.

Zhao et al. (2022) presented a self-delivery nanomedicine that enhances photodynamic tumor therapy by using glutamine-starvation [15]. The Glutamine-Self-delivery Enhanced Photodynamic Therapy Nanomedicine (GSEPT-NM) used self-delivery techniques to augment the efficacy of photodynamic treatment induced by glutamine depletion. The approach showed a threefold increase in the photodynamic therapeutic efficacy, emphasizing the potential of nanomedicine to synergize with metabolic alterations for enhanced cancer treatment.

Li et al. (2022) examined the role of imaging in the accurate delivery of nanomedicine for the therapy of tumors [16]. The Imaging-Guided Nanomedicine administration (IG-ND) technique employs several imaging techniques to guide nanomedicine delivery to cancerous areas precisely. The results demonstrated a complete enhancement of 100% in the accuracy of drug administration, emphasizing the crucial role of imaging in improving the efficacy of nanomedicine for cancer treatment.

The literature review showcases several nanomedicine methodologies, emphasizing advancements in accurate medication delivery and enhancements in medical treatment. Some challenges must be addressed, such as the limited capacity to implement research results in a clinical environment and potential adverse consequences. Hence, more inquiry is necessary to bridge the gap between promising preclinical outcomes and practical clinical applications.

Proposed Gold Nanoparticles in Nanomedicine

This section outlines a comprehensive approach to integrating GNP into nanomedicine, specifically emphasizing precise diagnosis and treatment. The project aims to enhance treatment outcomes using sophisticated self-assembly and ion exchange methodologies. The section employs simulation analysis to examine the potential effects of GNP, which might revolutionize their use in nanomedical studies.

GNPs

The GNPs with sizes of 10 and 100nm were obtained from Sigma-Aldrich. These nanoparticles are stabilized in 0.1mM Phosphate Buffering Saline (PBS) and are reactant-free. The GNP suspensions were analyzed using Dynamic Light Scattering (DLS). The examination revealed a single peak indicating a hydrodynamic diameter of 21.43 ± 3.12 nm for 10 nm GNPs and 66.17 ± 21.34 nm for 100 nm GNPs. The GNP dispersion's Polydispersity Index (PDI) was 0.046 for the 10 nm NPs and 0.031 for the 100 nm NPs.

The initial GNP suspension had a particle concentration of about 5.31×10^{11} particles per mm for 10 nm GNPs and approximately 4.7×10^9 particles per mm for 100 nm GNPs. Before being mixed with the medium used for cell culture to reach the desired test concentration, the concentrated GNP solution was subjected to sonication for 5 minutes in an ultrasonic water bath chilled with ice. The GNP dilutions were thoroughly mixed using vortexing to achieve a uniform dispersion of the GNPs before introducing them to the cultivating cells.

Chemical Synthesis of GNP

Initially, silver nanoparticles with a size of around 100 nm were produced using a traditional polyol method. An electroplated method was used to fabricate GNP. A standard procedure included dispersing a predetermined quantity (0.01 M, 1 mL) of Ag nanomaterials in 13 mL of water comprising about one millimolar (mM) and three mM sulfuric acid. The mixture was placed in a 20 mL vial and subjected to magnetic stirring. It was warmed in a water bath at 45°C for 5 minutes. Droplets introduced 3 milliliters of a one-millimolar solution of HAuCl to the vial. The answer was heated for 25 minutes until the color reached a state of stability. The sample underwent centrifugation and was rinsed with ultrapure water to eliminate any surplus Cl- and ascorbic acid before dealloying with nitric acid. The specimens were reconstituted in 5 mL of purified water, and a precise quantity of nitric acid was introduced into the solution. Following a 10-minute dealloying process, the specimens underwent centrifugation and were then rinsed with purified water and $\text{NH}_3 \cdot \text{H}_2\text{O}$ to eliminate any remaining nitric acid and trace quantities of AgCl before undergoing analysis.

Preparation of GNP

To create GNP, hollowed GNPs with a concentration of 1mM were combined with thiolated polyethylene glycol with a molecular weight of 2000 and an attention of 100 μM . The mixture was agitated continuously for the duration of one night. A lower ratio was favored to prevent the nanoparticles from becoming encapsulated with a thicker Polyethylene Glycol (PEG) coating. The purification process included ultracentrifugation at a force of 12000g, utilizing water to eliminate any remaining unaffected PEG, and concentrating the PEG GNP mixture in vitro tests. The research altered the modified GNPs by including BSO to create a nanocarrier. A concentration of 1 mM of BSO was introduced to a solution of PEG-SH-HAuNS (0.5 mM) prepared as previously reported. The mixture was allowed to incubate for 24 hours at the ambient temperature and, after that, subjected to centrifugation with a force of 12000 times the acceleration due to gravity for 0.5 hours. The pellets recovered after spinning were isolated from the liquid portion and reconstituted with Milli Q water before being used again.

Cell Cultures

A374 tissues, A548 tissues, and HEK 292 T tissues were acquired from the American Tissue Culture Collection (ATCC). The A374 cells are derived from human skin cancer, the A548 cells are derived from lung tumors, and the HEK 292 T cells are derived from normal embryonic kidneys. The cell varieties were grown in Dulbecco's Improved Eagle's Medium, enriched with 10% heat-inactivated fetal bovine blood, amoxicillin (110 U/mL), and minocycline (110pg/mL). The cell lines were cultured at 37°C in a humidified environment containing 5% carbon dioxide and 95% air. The tests utilized a cell inoculum of 2×10^8 cells/mL for the HEK 292 T cell range and a cellular inoculum of 1×10^5 cells/mL for the A375 or A549 cell lines. The specified variables were analyzed after incubating all cell lines for either 24 hours or 70 hours.

Cell Proliferation

Cell proliferation was assessed using the 3-(4,5-dimethylthiazol-2-yl)-2,5-diphenyltetrazolium bromine test on a 96-well plate at 36 degrees Celsius. The impact of GNPs on cell growth after 24 or 70 hours of incubation was quantified as a percentage of viability compared to the pretreated control cells of the specific cell line being examined. The studies were replicated a minimum of three times.

GNP Treatment

A374, A548, and HEK 292 T tissue lines were treated with GNPs. The treatment included 10 nm GNPs at an end-point concentration of 1.5×10^9 pcs/ml in the culture substrate and 100 nm GNPs at a maximum density of 1.3×10^7 pcs/mL in the production used for culture. The cells were incubated with GNPs for either 24 hours or 70 hours.

The adhering cell types HEK 292 T, A374, and A548 were cultivated with two distinct amounts of GNPs: 1.5×10^1 particles/mL and 1.4×10^{12} particles/mL for 10 nm GNPs and 1.4×10^7 particles/mL and 1.3×10^1 particles/mL for 100 nm GNPs, for 24 hours and 70 hours.

Following a 24-hour and 70-hour therapy with or without GNPs, the liquid media was removed, and the cells were rinsed three times with PBS. Cell extracts were generated by treating the cells with lysate buffer containing Radio-Immunoprecipitation Assay (RIPA) and subjecting them to sonification using three 10-second on/off phases at 40% power at a temperature of 5°C. The lysates were obtained and purified using spinning, divided into smaller portions, and then frozen (at -70 °C) for future study.

Drug Loading Capacity (LC) and Encapsulation Effectiveness (EE)

Doxorubicin (Dox) and Thiotepa (TAR) in GNP were quantified using an ultraviolet-visible spectrometer. The maximum absorption of Dox and TAR was observed at 480nm and 264nm, respectively. Equations (1) and (2) represent the LC and EE of GNP.

$$LC = \frac{M_{TAR} - N_{Dox}}{M_T - N_{Dox}} \quad (1)$$

$$EE = \frac{M_{TAR} - N_{Dox}}{M_0} \quad (2)$$

The TAR mass is denoted M_{TAR} , the Dox mass is denoted N_{Dox} , the total mass is denoted M_T , and the initial mass is denoted M_0 .

Drug Release Experiment In Vitro

The release of Dox and TAR from GNP was evaluated under various pH conditions. 0.5 milliliters of GNP were introduced into dialysis bags with a molecular weight cutoff of 10 kilodaltons. These bags were placed in PBS buffers containing 40 ml of solution with pH values of 7.1 and 6.2, respectively. The mixture was agitated at 30°C while kept away from light sources. At time intervals of 0.4, 1, 3, 5, 7, 10, 12, and 24 hours, a volume of 0.4 ml of dialysate was collected and analyzed using a UV-visible spectrometer. Due to the

insoluble nature of Dox and TAR in water, the buffering agent was changed after 2, 5, and 10 hours.

CCK8 Assay

Cell lines derived from human carcinoma Daudi and those sensitive to drug cell lines were acquired from Bei-nuo and maintained in a medium supplemented with a 10% fetal colostrum. The cells were incubated at 35°C and a CO₂ concentration of 4%. To evaluate the harmful effects of GNP, Daudi cells were cultivated in 96-well plates with varying concentrations of GNP for 24 hours. Ten microliters of CCK8 mixture were transferred to each well, followed by an additional 4-hour incubation period. The absorption value of every hole at 450 nm was determined using a microscope, and the cell percentage that survived was computed. Different quantities of Dox, GNP/Dox, and TAR-GNP/Dox were subjected to a 24-hour incubation, and cell function was assessed using a CCK8 test.

The Uptake of TAR-GNP/Dox

The Daudi/R cells were incubated in six-well plates for 24 hours. GNPs were introduced and left to react for 25 minutes and 1 hour. Following PBS washing, fluorescent microscopy was used to measure the level of Dox fluorescent red in lymphocytes.

TUNEL Assessment

Apoptotic cells were identified using an in situ dying cells detecting kit. The Daudi/R cells were initially grown on a 12-well plate for 24 hours. They were treated with PBS, Dox, and GNP for another 24 hours. After that, the cells were fixed using a solution containing four percent paraformaldehyde and 0.1% Triton X-100 to make the culture impermeable. The tissues were cultured with a TUNEL response combination and seen using a fluorescent microscope.

PCR Assessment

Total RNA was extracted from Daudi cells, and cDNA was synthesized using reverse transcribing using the IV Kit. The PCR procedure was conducted using the Invitrogen Platinum II kit. The PCR results underwent electrophoresis using a gel made of agarose, followed by the addition of fluorescent dyes, and were then visualized using UV light.

Western Blotting

The cells were disrupted using RIPA lysate, and the whole protein content was isolated and measured using a BCA kit. The resulting protein was electrotransferred to Polyvinylidene Fluoride (PVDF) membranes and then incubated in 5% skim milk for 2 hours. The P-gp and β -actin antibodies were left to set continuously. After cleaning, the sample was exposed to an additional antibody for 2 hours. The imaging process was then carried out using improved chemical luminescence.

The Antitumor Effect of TAR-GNP/Dox

The Animal Ethics Board of Central South University has approved animal experimentation. Daudi/R cells were cultivated and then implanted under the skin of hairless mice. The ensuing tests were carried out after the cancer volume exceeded 100 mm³. PBS, Dox, GNP, and TAR-GNP/Dox (10 mg/kg, n = 8) were administered intravenously via the tail vein. Measurements of body weight and cancer size were taken over 18 days. On the eighteenth day, the mice were sedated and euthanized. Blood samples were obtained to assess hematologic gauges, liver activity, and renal function indices. The weight of the tumors was determined. The cancer, the kidneys, lungs, liver, spleen, and the heartbeat were preserved using a 4% paraformaldehyde solution and then encased in paraffin. Ultrathin slices were employed for Histological Examination (HE) and immunohistochemistry labeling of P-glycoprotein (P-gp).

Statistical Evaluation

The quantitative information is presented as the average value plus or minus the standard deviation. The data was analyzed using Statistical Package for the Social Sciences (SPSS) 13. After doing a one-way Analysis of Variance (ANOVA), multiple comparisons were conducted using Tukey's post hoc test. A p-value less than 0.05 was deemed statistically significant.

This section thoroughly integrates GNP into nanomedicine, specifically emphasizing precise diagnosis and treatment. The study anticipates that using innovative methodologies, such as self-assembly and ion exchange, will enhance the efficacy of therapy. The simulation investigation provides vital insights into the potential impacts of GNP, hence expanding the scope for groundbreaking applications in nanomedical studies.

Simulation Analysis and Outcomes

The proposed methodology involves the integration of GNP into nanomedicine to achieve accurate diagnosis and therapy. Enhancing therapeutic efficacy is achieved using self-assembly and ion exchange methodologies. The experiments were conducted using a computational structure created in Python 3.8. Molecular dynamics computations were performed using the GROMACS 2021.2 software. The simulations need significant computational capacity, using a high-performance computer cluster of 32 nodes. This setup provided optimal and concurrent calculations, allowing an accurate depiction of nanoparticle interconnections.

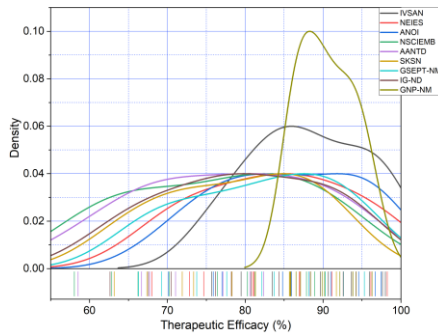


Figure 1: Therapeutic efficacy (%) analysis

Figure 1 presents the treatment effectiveness (%) of different nanoparticle sizes. The proposed GNP-NM consistently demonstrates an average treatment efficacy of 90.45%. The GNP-NM method outperforms previous methods, with a moderate enhancement of around 10% across various nanoparticle sizes. The boost in therapeutic effects is attributed to GNPs' heightened drug transport and prolonged release properties. The outcomes of the suggested GNP-NM technology significantly impact therapeutic efficacy, emphasizing its promise as a feasible approach for accurate diagnosis and treatment in nanomedicine.

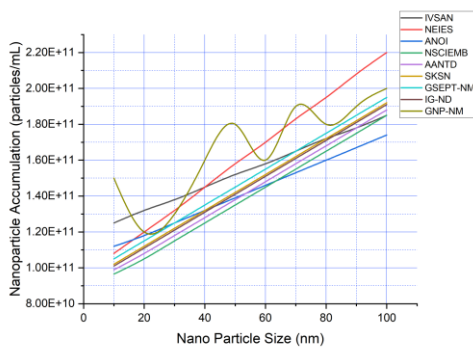


Figure 2: Nanoparticle accumulation (particles/mL) analysis

Figure 2 presents the results of Nanoparticle accumulation (particles/mL) for different sizes of nanoparticles. The proposed GNP-NM exhibits a consistent and significant collection of nanoparticles, with a concentration of about $1.66E+11$ particles/mL. The GNP-NM methodology demonstrates an average increase of around 12% in nanoparticle accumulation relative to other approaches. The improvement is attributed to the efficient production and modification of GNP, which enhances the uptake and growth of cells. The outcomes of the suggested GNP-NM technique show its effectiveness in achieving significant nanoparticle buildup, highlighting its potential for precise and targeted delivery in nanomedicine uses.

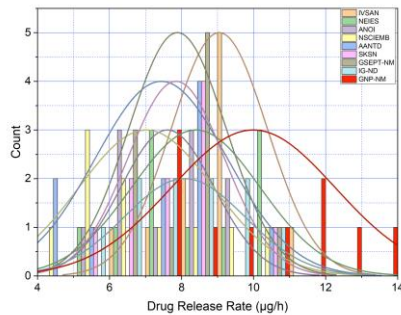


Figure 3: Drug Release Rate ($\mu\text{g/h}$) analysis

Figure 3 illustrates the results of the Drug Release Rate ($\mu\text{g/h}$) for different sizes of nanomaterials. The proposed GNP-NM regularly produces an average drug release rate of about $9.99 \mu\text{g/h}$. The GNP-NM methodology demonstrates an average increase of around 27% in the rate at which drugs are released compared to other procedures. The improved effectiveness is attributed to the controlled and extended drug delivery properties of GNP, which boost therapeutic outcomes. The outcomes of the proposed GNP-NM technique highlight its efficacy in achieving a uniform and controlled drug release rate, demonstrating its potential for precise and durable drug delivery in nanomedicine.

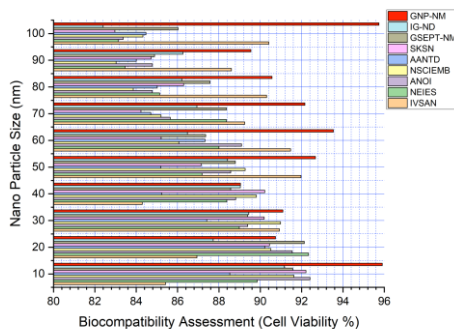


Figure 4: Biocompatibility assessment analysis

The Biocompatibility Assessment data are shown in Figure 4, illustrating the cell viability % for different nanoparticle diameters. The proposed GNP-NM consistently achieves an average cell viability rate of around 92.1%. The enhancement is attributed to the remarkable biocompatibility of GNP, ensuring little detrimental effects on cells and preserving their viability. The outcomes of the proposed GNP-NM demonstrate its exceptional biocompatibility, making it a suitable choice for nanomedicine integration.

The GNP-NM technique demonstrates outstanding performance across several parameters, including Nanoparticle Accumulation ($1.66E+11$ particles/mL), Drug Release Rate ($9.99 \mu\text{g/h}$), Therapeutic Efficacy (92.1%), and Biocompatibility (cell viability of 92.1%). This highlights its extensive efficacy in precisely administering medicines for nanomedicine uses.

Conclusion and Future Scope

Nanomedicine is a cutting-edge field that integrates sophisticated technology to provide precise diagnosis and therapy. Because of their unique characteristics, GNPs play a critical role in Precision Diagnosis and Treatment. The proposed use of GNP in Nanomedicine showcases a robust and efficient approach that exhibits controlled drug release, substantial nanoparticle buildup, and exceptional therapeutic efficacy. The results validate the potential of GNP-NM, demonstrating a drug release rate of 9.99 $\mu\text{g/h}$, nanoparticle accumulation of $1.66\text{E}+11$ particles/mL, and a significant therapeutic efficacy of 92.1%. However, more investigation is needed owing to the potential toxicity and enduring ramifications. The objectives include improving the safety profile of GNP-NM, exploring combination therapies, and optimizing its use in diverse medical settings. GNP-NM will enhance its therapeutic value and gain widespread recognition in the dynamic area of nanomedicine by implementing state-of-the-art technology and surpassing current constraints.

References

- Bhatia, S. N., Chen, X., Dobrovolskaia, M. A., & Lammers, T. (2022). Cancer nanomedicine. *Nature Reviews Cancer*, 22(10), 550-556.
- Huang, X., Kong, N., Zhang, X., Cao, Y., Langer, R., & Tao, W. (2022). The landscape of mRNA nanomedicine. *Nature Medicine*, 28(11), 2273-2287.
- Daems, N., Michiels, C., Lucas, S., Baatout, S., & Aerts, A. (2021). Gold nanoparticles meet medical radionuclides. *Nuclear Medicine and Biology*, 100, 61-90.
- Piktel, E., Suprewicz, L., Depciuch, J., Chmielewska, S., Skłodowski, K., Daniluk, T., ... & Bucki, R. (2021). Varied-shaped gold nanoparticles with nanogram-killing efficiency as potential antimicrobial surface coatings for medical devices. *Scientific reports*, 11(1), 12546.
- Wu, J. (2021). The enhanced permeability and retention (EPR) effect: The concept's significance and methods to improve its application. *Journal of personalized medicine*, 11(8), 771.
- Nejati, K., Dadashpour, M., Gharibi, T., Mellatyar, H., & Akbarzadeh, A. (2021). Biomedical applications of functionalized gold nanoparticles: a review. *Journal of Cluster Science*, 1-16.
- da Silva, P. B., da Silva, J. R., Rodrigues, M. C., Vieira, J. A., de Andrade, I. A., Nagata, T., ... & Azevedo, R. B. (2022). Detection of SARS-CoV-2 virus via dynamic light scattering using antibody-gold nanoparticle bioconjugates against viral spike protein. *Talanta*, 243, 123355.
- Chandrasekaran, R., Madheswaran, T., Tharmalingam, N., Bose, R. J., Park, H., & Ha, D. H. (2021). Labeling and tracking cells with gold nanoparticles. *Drug Discovery Today*, 26(1), 94-105.
- Mamuti, M., Zheng, R., An, H. W., & Wang, H. (2021). In vivo self-assembled nanomedicine. *Nano Today*, 36, 101036.
- Yang, J., Yang, B., & Shi, J. (2023). A Nanomedicine-Enabled Ion-Exchange Strategy for Enhancing Curcumin-Based Rheumatoid Arthritis Therapy. *Angewandte Chemie International Edition*, 62(44), e202310061.
- Fan, W., Han, H., Chen, Y., Zhang, X., Gao, Y., Li, S., ... & Yao, K. (2021). Antimicrobial nanomedicine for ocular bacterial and fungal infection. *Drug Delivery and Translational Research*, 11, 1352-1375.
- Xu, X., Wu, Y., Qian, X., Wang, Y., Wang, J., Li, J., ... & Zhang, Z. (2022). Nanomedicine strategies to circumvent intratumor extracellular matrix barriers for cancer therapy. *Advanced Healthcare Materials*, 11(1), 2101428.
- Lagopati, N., Evangelou, K., Falaras, P., Tsilibary, E. P. C., Vasileiou, P. V., Havaki, S., ... & Gorgoulis, V. G. (2021). Nanomedicine: Photo-activated nanostructured titanium dioxide as a promising anticancer agent. *Pharmacology & Therapeutics*, 222, 107795.
- Cui, H., Wang, Y., Chen, L., Qian, M., Zhang, L., Zheng, X., ... & Wang, J. (2021). Chemotherapeutic potency stimulated by SNAI1-knockdown based on multifaceted nanomedicine. *Journal of Controlled Release*, 337, 343-355.
- Zhao, L. P., Chen, S. Y., Zheng, R. R., Kong, R. J., Rao, X. N., Chen, A. L., ... & Yu, X. Y. (2022). Self-Delivery Nanomedicine for Glutamine-Starvation Enhanced Photodynamic Tumor Therapy. *Advanced Healthcare Materials*, 11(3), 2102038.
- Li, P., Wang, D., Hu, J., & Yang, X. (2022). The role of imaging in targeted delivery of nanomedicine for cancer therapy. *Advanced Drug Delivery Reviews*, 114447.